AIAA JOURNAL
Vol. 35, No. 8, August 1997

Application of Nonlinear Localization to the Optimization of a Vibration Isolation System

Tariq A. Nayfeh,* Edward Emaci,* and Alexander F. Vakakis†
University of Illinois at Urbana–Champaign, Urbana, Illinois 61801

We consider a passive nonlinear mechanical vibration isolator consisting of discrete mass, stiffness, and damping elements. We show that, by suitably designing the stiffness nonlinearities, we can induce localized nonlinear normal modes (NNMs) in this system. These are unforced oscillations analogous to the normal modes of classical linear vibration theory, with energies that are spatially confined. When the isolator with localized NNMs is subjected to harmonic excitations in certain frequency ranges, the resulting resonances become similarly localized and the level of the transmitted undesirable vibrations is greatly reduced. Hence, nonlinear localization can provide a valuable tool for developing improved vibration and shock isolation designs, otherwise unattainable using linear theory. In addition, we develop a technique that systematically optimizes the localized NNMs of the unforced isolator, by localizing the vibrational energy in a way that is compatible to the vibration isolation objectives. This ensures minimal transfer of unwanted disturbances when a harmonic excitation is applied to the system.

Introduction

In many engineering applications involving vibrating machinery, there is a need to reduce the vibration level to conform with performance objectives. For example, considering the vibrations of a spacecraft induced by spinning momentum flywheels, if the level of the disturbances that are transmitted to the main body of the spacecraft are above a certain threshold, they may adversely affect the ability of performance objectives, such as the precision pointing of sensitive devices. Hence, it is desirable to minimize the transfer of unwanted vibrations to the structure over the specified frequency ranges of interest.

Traditional techniques for preventing the transfer of vibrational energy from components to the structure include the use of elastomers,[1] vibration isolation paddings, damping tapes, springs, rubber mounts and cork padding,[2–4] passive vibration absorbers,[5,6] and, in many instances, active controllers.[5,7,8] Base isolation systems are also used in order to prevent the transfer of seismic energy into buildings. The majority of such systems are designed so that the isolators are flexible and the structure is quite stiff, and the vibrational energy is dissipated through the use of dampers. Such systems, in addition to preventing damage to the building, are also thought to prevent damage to internal components.[9]

We propose a new design technique for vibration isolation based on the concept of nonlinear normal mode (NNM).[10–12] The passive vibration isolation element is not regarded as an external addition to the system, but rather an integral part of the casing of the vibrating component. Stiffness nonlinearities are then used to induce nonlinear mode localization,[11,13,14] thus confining the vibrational energy[15] away from the main body to be isolated. In contrast with previously studied nonlinear vibration absorbers,[16,17] the present technique implements nonlinear mode localization for vibration isolation and formulates a design methodology for inducing optimum nonlinear localization properties in the vibration isolation system.

Mathematical Model

The simplified model of the vibration isolation system considered is shown in Fig. 1. It consists of the vibrating component (mass m_1) located in a case (mass m_2) that is attached to an intermediate grounding mass (m_3). The intermediate mass is connected to the structure to be isolated. Following the aforementioned example, mass m_1 would be a simplified model of a spinning momentum flywheel that is enclosed in a case represented by mass m_2. The case is, in turn, attached to the supporting mass m_3 that is connected to the main body of the spacecraft. The combination of masses m_1 and m_2 will be referred to as the upper substructure (USS), whereas mass m_3 will be referred to as the lower substructure (LSS). In addition, such a structure can be thought of as a reverse base isolation system, where instead of preventing the ground vibrations from affecting the structure, the structure's vibrations are prevented from affecting the ground.

In the system of Fig. 1, the attachment of mass m_1 to mass m_2 is through a general nonlinear stiffness denoted as $f(y)$ and a linear viscous damper denoted by c_1. Mass m_2 is connected to mass m_3 by means of the linear stiffness k and the linear damper c_2. Finally, mass m_3 is grounded to the main structure by the nonlinear stiffness $g(y)$ and the linear damper c_3. The displacement of mass m_i is denoted by x_i, and the equations of motion assume the form

$$\begin{aligned} &m_1\ddot{x}_1 + c_1(\dot{x}_1 - \dot{x}_2) + f(x_1 - x_2) = P(t)\\ &m_2\ddot{x}_2 + c_1(\dot{x}_2 - \dot{x}_1) + f(x_2 - x_1) + \bar{k}(x_2 - x_3) + c_2(\dot{x}_2 - \dot{x}_3) = 0\\ &m_3\ddot{x}_3 + c_3\dot{x}_3 + c_2(\dot{x}_3 - \dot{x}_2) + g(x_3) + \bar{k}(x_3 - x_2) = 0 \end{aligned} \quad (1)$$

where the dot represents the derivative with respect to time and $P(t)$ denotes the external excitation applied to the USS.

We begin by demonstrating that localized vibrations can exist in this system, and we show the effects on the dynamics of increasing the order of the nonlinearities. Then, we introduce a new design methodology by which an optimized nonlinear localized mode is induced in this system for the purpose of vibration isolation. We analyze the dynamics of Eqs. (1) using two different approaches based on the methods of multiple scales and harmonic balance.[18,19] The aim of the analysis is to show that, by suitable design of the linear and nonlinear coefficients, we can induce localized NNMs in the system and improve its vibration isolation properties over wide frequency ranges.

Analysis by the Method of Multiple Scales

We first study the nonlinear localization properties of system (1) using the method of multiple scales. This enables us to obtain a set of modulation equations governing the time evolution of the amplitudes and phases of the system's response. We introduce the following parametrizations for the nonlinear stiffnesses:

$$f(y) = f_1 y + \varepsilon f_m y^m \qquad \text{and} \qquad g(y) = g_1 y + \varepsilon g_n y^n \quad (2)$$

where m and n are odd integers and $|\varepsilon| \ll 1$ is a small parameter denoting the smallness of the nonlinear stiffness coefficients. The

Received April 4, 1996; revision received Feb. 2, 1997; accepted for publication April 22, 1997.

*Graduate Research Assistant, Department of Mechanical and Industrial Engineering, 1206 West Green Street.

†Associate Professor, Department of Mechanical and Industrial Engineering, 1206 West Green Street.

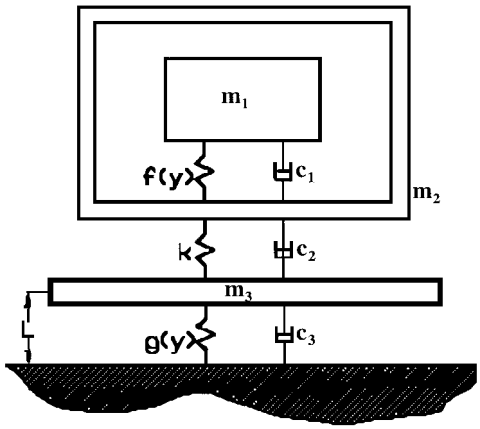

Fig. 1 Model under consideration.

introduction of the small parameter in the problem is necessary to perform the perturbation analysis that follows. Furthermore, we introduce the coordinate transformations $u = x_1 - x_2$, $v = m_1x_1 + m_2x_2$, and $w = x_3$. Here u represents the relative motion of mass m_1 with respect to mass m_2, v is a scaled motion of the center of mass of the USS, and w denotes the motion of the LSS. The aim of the analysis is to render w as small as possible to achieve small transmission of vibration to the main body of the system. Using the preceding coordinate transformations, introducing the new nondimensional time variable $\tau = (\mu_1 f_1)^{1/2}t \equiv \omega t$, where $\mu_1 = [(m_1+m_2)/m_1m_2]$, and rescaling u as $u \to u(f_m/f_1)^{1/(m-1)}$, we express the equations of motion in the following nondimensional form:

$$\begin{aligned}
&\ddot{u} + u + \varepsilon\left[u^m + k_{11}v + k_{12}u + k_{13}w + d_{11}\dot{u} + d_{12}\dot{v} + d_{13}\dot{w}\right] \\
&\quad = (\varepsilon F/m_1\omega^2)(f_m/f_1)^{-1/(m-1)}\cos[(\omega/\omega)\tau] \\
&\ddot{v} + \varepsilon\left[k_{21}v + k_{22}u + k_{23}w + d_{21}\dot{v} + d_{22}\dot{u} + d_{23}\dot{w}\right] \\
&\quad = (\varepsilon F/\omega^2)\cos[(\omega/\omega)\tau] \qquad (3) \\
&\ddot{w} + (1+\varepsilon\lambda)w \\
&\quad + \varepsilon\left[w^n + k_{31}v + k_{32}u + k_{33}w + d_{31}\dot{w} + d_{32}\dot{u} + d_{33}\dot{v}\right] = 0
\end{aligned}$$

where the force $P(t) = \varepsilon F\cos(\omega\tau)$ acting on mass m_1 is assumed to be harmonic and of small amplitude and the coefficients in Eqs. (3) are defined as follows:

$$k_{11} = -\frac{k}{m_1m_2^2\mu_1\omega^2}a, \qquad k_{12} = \frac{k}{m_2^2\mu_1\omega^2}, \qquad k_{13} = \frac{k}{m_2\omega^2}a$$

$$d_{11} = \frac{1}{\omega}\left(c_1\mu_1 + c_2\frac{1}{m_2^2\mu_1}\right)$$

$$d_{12} = -\frac{c_2}{m_1m_2^2\mu_1\omega}a, \qquad d_{13} = \frac{c_2}{m_2\omega}a, \qquad k_{21} = \frac{k}{m_1m_2\mu_1\omega^2}$$

$$k_{22} = -\frac{k}{m_2\mu_1\omega^2}\frac{1}{a}, \qquad k_{23} = -\frac{k}{\omega^2}, \qquad a = \left(\frac{f_m}{f_1}\right)^{-1/(m-1)}$$

$$d_{21} = \frac{c_2}{m_1m_2\mu_1\omega}, \qquad d_{22} = -\frac{c_2}{m_2\mu_1\omega}\frac{1}{a}, \qquad d_{23} = -\frac{c_2}{\omega}$$

$$g_1 = m_3\omega^2(1+\varepsilon\lambda), \qquad k_{31} = -\frac{k}{m_1m_2m_3\mu_1\omega^2}$$

$$k_{32} = \frac{k}{m_2m_3\mu_1\omega^2}\frac{1}{a}, \qquad k_{33} = \frac{k}{m_3\omega^2}, \qquad g_n = m_3\omega^2$$

$$d_{31} = \frac{(c_2+c_3)}{m_3\omega}, \qquad d_{32} = \frac{c_2}{m_2m_3\mu_1\omega}\frac{1}{a}$$

$$d_{33} = -\frac{c_2}{m_1m_2m_3\mu_1\omega}, \qquad \bar{k} = \varepsilon k$$

Differentiation in Eqs. (3) is now with respect to the new time variable τ. We note that the parameter λ in the preceding relations provides a measure of the detuning between the linear frequency of the relative motion and the linear frequency of the intermediate mass, whereas the parameter a is a measure of the relative strength of the nonlinear vs the linear coefficient in $f(y)$.

For $\varepsilon = 0$, Eqs. (3) represent two uncoupled linear oscillators with identical natural frequencies equal to unity and a rigid body motion governed by v. We now study the response of Eqs. (3) for small (but nonzero) ε. To this end, we introduce the new scaled time variable $\hat{t} = \bar{\omega}\tau$ and the following relation for the frequency of the harmonic excitation:

$$\bar{\omega} = \omega/\omega = 1 + \varepsilon\sigma \qquad (4)$$

where σ is a frequency detuning parameter. Relation (4) represents a challenging vibration isolation problem because the forcing frequency is assumed to be in the neighborhood of the two linearized natural frequencies of Eqs. (3). Under such conditions, large-amplitude oscillations are anticipated for w and the problem of vibration isolation is challenging. However, as we show subsequently, even under such demanding conditions, nonlinear localization can provide a valuable tool for ensuring small steady-state responses of w over wide frequency ranges.

Taking into account Eq. (4), applying the chain rule of differentiation, and keeping terms only up to $\mathcal{O}(\varepsilon)$, we rewrite the equations of motion as

$$\begin{aligned}
&u'' + u + \varepsilon\left[2\sigma u'' + u^m + k_{11}v + k_{12}u + k_{13}w + d_{11}u'\right. \\
&\quad \left. + d_{12}v' + d_{13}w'\right] = \varepsilon B\cos(\hat{t}) \\
&v'' + \varepsilon\left[2\sigma v'' + k_{21}v + k_{22}u + k_{23}w + d_{21}v' + d_{22}u' + d_{23}w'\right] \\
&\quad = (\varepsilon F/\omega)\cos(\hat{t}) \qquad (5) \\
&w'' + (1+\varepsilon\lambda)w + \varepsilon\left[2\sigma w'' + w^n + k_{31}v + k_{32}u + k_{33}w\right. \\
&\quad \left. + d_{31}w' + d_{32}u' + d_{33}v'\right] = 0, \qquad B = (F/m_1\omega^2)\alpha
\end{aligned}$$

where primes denote differentiation with respect to the new time $\hat{t} = \omega\tau$. Applying the method of multiple time scales,[18] we expand u, v, and w in the following form:

$$\begin{aligned}
u(\hat{t}) &= u_0(T_0, T_1, \ldots) + \varepsilon u_1(T_0, T_1, \ldots) + \ldots \\
v(\hat{t}) &= v_0(T_0, T_1, \ldots) + \varepsilon v_1(T_0, T_1, \ldots) + \ldots \qquad (6) \\
w(\hat{t}) &= w_0(T_0, T_1, \ldots) + \varepsilon w_1(T_0, T_1, \ldots) + \ldots
\end{aligned}$$

where the slow and fast time scales are defined as $T_i = \varepsilon^i\hat{t}$. The derivatives in Eqs. (5) are expressed with respect to the slow and fast time scales as

$$\frac{d(\,)}{d\hat{t}} = D_0 + \varepsilon D_1 \qquad \text{and} \qquad \frac{d^2(\,)}{d\hat{t}^2} = D_0^2 + 2\varepsilon D_0D_1 + \mathcal{O}(\varepsilon^2) \qquad (7)$$

where $D_i = \partial(\,)/\partial T_i$. Substituting Eqs. (6) and (7) into Eqs. (5) and setting the coefficients of like powers of ε equal to zero, we obtain a series of subproblems governing successive orders of approximation.

The leading-order approximation to the dynamic responses are governed by the following linear equations that are obtained by considering the $\mathcal{O}(\varepsilon^0)$ terms in Eqs. (5):

$$\begin{aligned}
D_0^2u_0 + u_0 &= 0 \\
D_0^2v_0 &= 0 \qquad (8) \\
D_0^2w_0 + w_0 &= 0
\end{aligned}$$

The solutions of this set are given by

$$\begin{aligned}
u_0(T_0, T_1) &= A(T_1)e^{jT_0} + \bar{A}(T_1)e^{-jT_0} \\
v_0(T_0, T_1) &= B_1(T_1)T_0 + B_2(T_1) \qquad (9) \\
w_0(T_0, T_1) &= C(T_1)e^{jT_0} + \bar{C}(T_1)e^{-jT_0}
\end{aligned}$$

where A, C, and B_i are complex functions of the slow time scale T_1 and the overbar represents the complex conjugate. These slowly varying functions are computed by proceeding to the next order of approximation taking into account $\mathcal{O}(\varepsilon^1)$ terms in Eqs. (5),

$$\begin{aligned}
&D_0^2u_1 + u_1 = -2D_0D_1u_0 - k_{12}u_0 - 2\sigma D_0^2u_0 - k_{11}v_0 - k_{13}w_0\\
&\quad - u_0^m - d_{11}D_0u_0 - d_{12}D_0v_0 - d_{13}D_0w_0 + B\cos(T_0)\\
&D_0^2v_1 = -k_{22}u_0 - 2D_0D_1v_0 - 2\sigma D_0^2v_0 - k_{21}v_0 - k_{23}w_0\\
&\quad - d_{22}D_0u_0 - d_{21}D_0v_0 - d_{23}D_0w_0 + (F/\alpha^2)\cos(T_0)\\
&D_0^2w_1 + w_1 = -k_{32}u_0 - k_{31}v_0 - 2D_0D_1w_0 - k_{33}w_0\\
&\quad - 2\sigma D_0^2w_0 - w_0^n - \lambda_1 w_0 - d_{32}D_0u_0 - d_{33}D_0v_0 - d_{31}D_0w_0
\end{aligned} \tag{10}$$

Substituting the solutions of the linear system (9) into Eqs. (10) and simplifying yields

$$\begin{aligned}
&D_0^2u_1 + u_1 = \left[-2jA' - (k_{12} - 2\sigma + jd_{11})A - (k_{13} + jd_{13})C\right.\\
&\quad \left. - m_f A^{(m+1)/2}\bar{A}^{(m-1)/2} + (aF/2)\right]e^{jT_0} + \text{cc}\\
&\quad - k_{11}(B_1T_0 + B_2) - d_{12}B_1 + \text{NST}\\
&D_0^2v_1 = [-k_{22}A - jd_{22}A - k_{23}C - jd_{23}C + (m_1f/2)]e^{jT_0}\\
&\quad + \text{cc} - 2B_1' - k_{21}(B_1T_0 + B_2) - d_{21}B_1\\
&D_0^2w_1 + w_1 = \left[-2jC' - (k_{33} - 2\sigma + jd_{31} + \lambda)C\right.\\
&\quad \left. - (k_{32} + jd_{32})A - n_f C^{(n+1)/2}\bar{C}^{(n-1)/2}\right]e^{jT_0} + \text{cc}\\
&\quad - k_{31}(B_1T_0 + B_2) - d_{33}B_1 + \text{NST}
\end{aligned} \tag{11}$$

where

$$m_f = \frac{m!}{[(m+1)/2]!\,[(m-1)/2]!}$$

$$n_f = \frac{n!}{[(n+1)/2]!\,[(n-1)/2]!}$$

and where cc stands for the complex conjugate of the preceding terms and NST stands for nonsecular terms.[18,19] To ensure that the series in Eqs. (7) is uniformly valid for all times $\hat{t}$, the terms B_1, B_2, and the secular terms in Eqs. (11), i.e., the terms on the right-hand sides that lead to unbounded responses, must be set equal to zero. Hence, we obtain the following set of solvability conditions governing the slow time evolutions of the complex amplitudes:

$$\begin{aligned}
&-2jA' - (k_{12} - 2\sigma + jd_{11})A - (k_{13} + jd_{13})C\\
&\quad - m_f A^{(m+1)/2}\bar{A}^{(m-1)/2} + (B/2) = 0\\
&\qquad B_1(T_1) = B_2(T_1) = 0\\
&-2jC' - (k_{33} - 2\sigma + jd_{31} + \lambda)C - (k_{32} + jd_{32})A\\
&\quad - n_f C^{(n+1)/2}\bar{C}^{(n-1)/2} = 0
\end{aligned} \tag{12}$$

from which we conclude that $v_0 = 0$. Introducing the polar representation

$$A(T_1) = \tfrac{1}{2}a_1(T_1)e^{j\beta_1(T_1)} \qquad \text{and} \qquad C(T_1) = \tfrac{1}{2}a_3(T_1)e^{j\beta_3(T_1)} \tag{13}$$

where $a_i(T_1)$ and $\beta_i(T_1)$ are real functions of T_1, into Eqs. (12) and separating into real and imaginary parts, we obtain the following set of modulation equations governing the amplitudes and phases:

$$\begin{aligned}
&a_1' + \tfrac{1}{2}k_{13}a_3\sin\gamma + \tfrac{1}{2}d_{11}a_1 + \tfrac{1}{2}d_{13}a_3\cos(\beta_3 - \beta_1) + (B/2)\sin\beta_1 = 0\\
&\quad a_3' - \tfrac{1}{2}k_{32}a_1\sin\gamma + \tfrac{1}{2}d_{31}a_3 + \tfrac{1}{2}d_{32}a_1\cos(\beta_3 - \beta_1) = 0\\
&-a_1\beta_1' + \tfrac{1}{2}k_{12}a_1 - \sigma a_1 + \tfrac{1}{2}k_{13}a_3\cos(\beta_3 - \beta_1) + m_f(a_1/2)^m\\
&\quad -\tfrac{1}{2}d_{13}a_3\sin(\beta_3 - \beta_1) - (B/2)\cos\beta_1 = 0\\
&-a_3\beta_3' + \tfrac{1}{2}k_{33}a_3 - \sigma a_3 + \tfrac{1}{2}k_{32}a_1\cos(\beta_3 - \beta_1) + n_f(a_3/2)^n\\
&\quad + \tfrac{1}{2}d_{32}a_1\sin(\beta_3 - \beta_1) + \tfrac{1}{2}\lambda a_3 = 0
\end{aligned} \tag{14}$$

First, we investigate the structure of the NNMs of the undamped and unforced system. These nonlinear oscillations are analogous to the normal modes of classical linear vibration theory and correspond to synchronous motion of the system.[11] The study of the NNMs of the system is performed for two main reasons: 1) to demonstrate that the system of Fig. 1 can be designed to possess localized NNMs with corresponding energies mainly confined to the USS and away from the LSS (which we want to isolate) and 2) to gain an understanding of the structure of the resonance curves of the forced and damped system. Indeed, the nonlinear resonances of the forced and damped system are expected to occur in neighborhoods of NNMs,[11] in direct similarity to linear vibration theory.

Hence, we set the c_i and P (or equivalently, the d_{ij} and F) equal to zero in Eqs. (14), which yields

$$a_1' + \tfrac{1}{2}k_{13}a_3\sin\gamma = 0 \tag{15a}$$

$$a_3' - \tfrac{1}{2}k_{32}a_1\sin\gamma = 0 \tag{15b}$$

$$\begin{aligned}
&a_1a_3\gamma' - \tfrac{1}{2}a_1a_3(k_{33} - k_{12}) - \tfrac{1}{2}\lambda_1a_1a_3 + m_fa_3(a_1/2)^m\\
&\quad - n_fa_1(a_3/2)^n + \tfrac{1}{2}(k_{13}a_3^2 - k_{32}a_1^2)\cos\gamma = 0
\end{aligned} \tag{15c}$$

where $\gamma = \beta_3 - \beta_1$. This is an autonomous system of equations whose stationary solutions (corresponding to $a_1' = a_3' = \gamma' = 0$) yield the $\mathcal{O}(1)$ approximations to the NNMs of the unforced and undamped system.

Combining Eqs. (15a) and (15b), we obtain the relations

$$k_{32}a_1'a_1 + k_{13}a_3'a_3 = 0 \Rightarrow k_{32}a_1^2 + k_{13}a_3^2 = \rho^2$$

or

$$a_1^2\left[k_{32} + k_{13}c^2\right] = \rho^2 \tag{16}$$

where ρ^2 is a constant of integration representing the (conserved) energy of the undamped unforced system and $c = a_3/a_1$. Imposing the stationary conditions on Eqs. (15), we obtain the following equation governing the ratio of the amplitudes a_3 and a_1 on a nonlinear normal mode of the system:

$$\begin{aligned}
&\left\{\lambda_1 + k_{33} - k_{12} \pm [k_{32}(1/c) - k_{13}c]\right\}(k_{32} + k_{13}c^2)^{(m-1)/2}\\
&\quad + n_f(\tfrac{1}{2}\rho c)^{n-1}(k_{32} + k_{13}c^2)^{(m-n)/2} - m_f(\tfrac{1}{2}\rho)^{m-1} = 0\\
&\qquad \gamma = k\pi, \qquad k = 0, 1, 2, \ldots
\end{aligned} \tag{17}$$

Defining

$$L = \frac{\lambda + k_{33} - k_{12}}{k_{32}}, \qquad \mu = \frac{m_3(m_1 + m_2)}{m_1m_2} \times \left(\frac{f_m}{f_1}\right)^{-2/(m-1)}$$

and

$$\eta = \frac{\rho}{k_{32}}$$

and noting that $k_{13} = \mu a^2 k_{32}$, we rewrite expression (17) in the following nondimensional form:

$$\begin{aligned}
&[cL \pm (1 - \mu a^2c^2)](1 + \mu a^2c^2)^{(m-1)/2} + n_f(\eta/2)^{(n-1)}k_{32}^{(n-3)/2}\\
&\quad \times c^n(1 + \mu a^2c^2)^{(m-n)/2} - m_f(\eta/2)^{(m-1)}k_{32}^{(m-3)/2}c = 0\\
&\qquad \gamma = k\pi, \qquad k = 0, 1, 2, \ldots
\end{aligned} \tag{18}$$

Equation (18) governs [correct to $\mathcal{O}(1)$] the ratios of the amplitudes of u and w on an NNM of the unforced and undamped system of Fig. 1. Regarding the parameters in Eq. (18), L is a nondimensional structural detuning, μ is a nondimensional mass ratio, and η is a nonlinearity to coupling ratio (because the strength of the nonlinearities of the system is a function of the level of energy ρ and k_{32} is a nondimensional coupling stiffness). Based on the preceding analysis, the + and − signs in Eq. (18) correspond to even or odd multiples of π for γ.

In Fig. 2a, we graphically depict the amplitude ratio c vs the detuning parameter L for $k_{32} = 1$, $m = n = 3$, $\mu = 1$, and varying values of η (without loss of generality, the phase difference is set

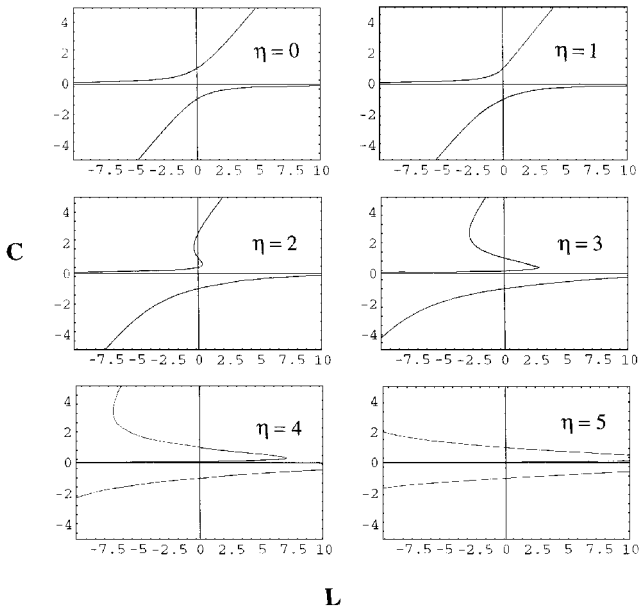

a) Dependence of the modal ratio c on η

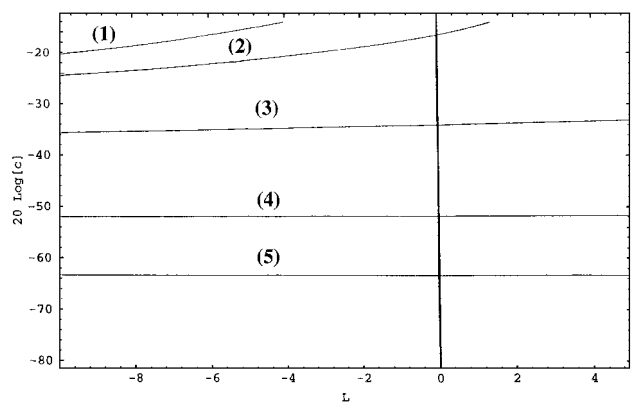

b) Dependence of c on the degrees of nonlinearity m and n for the strongly localized NNM

Fig. 2 NNMs of the system: a) $m = 3$, $n = 3$, $\mu = 1$, $k_{32} = 1$ and b) (1), $m = 0$ and $n = 0$ (linear case); (2), $m = 3$ and $n = 3$; (3), $m = 5$ and $n = 3$; (4), $m = 7$ and $n = 3$; and (5), $m = 9$ and $n = 3$.

equal to $\gamma = 0$). Note that the ratio of the nonlinearity to the coupling parameter greatly affects the structure of the NNMs of the system: for $\eta = 0$ (the linear case) the system possesses the linear normal modes, whereas for increasing η, a bifurcation occurs and the system possesses four NNMs. For negative values of L and large η, one branch of NNMs becomes strongly localized to the USS of the system because it corresponds to small values of c. Although such a localization occurs also in the linear system (with $\eta = 0$), the stiffness nonlinearities greatly enhance it. This is shown in Fig. 2b, where the aforementioned localized branch is depicted in a decibel scale for $k_{32} = 1$, $\mu = 5$, $\eta = 3$, and various degrees of USS and LSS stiffness nonlinearities m and n ($m = n = 0$ corresponds to the linear system). A perturbation analysis shows that for the localized NNM branch c is approximately given by

$$c \approx \frac{1}{L - m_f(\frac{1}{2})^{m-1} k_{32}^{(m-3)/2} \eta^{n-1}}$$

which depends on the nonlinearity of the USS. From Fig. 2b we note that as m and n increase the localization greatly increases. Moreover, the strength of localization depends mainly on the degree of nonlinearity n of the USS and not so much on the nonlinearity of the LSS. As a result, the motion is spatially confined to the USS, and the oscillation of the LSS becomes negligibly small. It is evident that such a localized NNM guarantees enhanced vibration isolation for the nonlinear system compared to the linear one.

The preceding results demonstrate that the system under consideration can be designed to possess a localized NNM with vibrational energy mainly confined to the USS and away from the main body to be isolated. As will be shown, the localized NNM gives rise to localized resonances of the forced and damped system and, thus, to improved vibration isolation of the system under periodic forcing. Reconsider Eqs. (14) with nonzero c_i and F. The nonlinear resonances of the system are obtained by imposing the stationarity conditions $a_1' = a_3' = 0$ and $\beta_1' = \beta_3' = 0$, which are necessary for steady-state periodic oscillations of the system. The resulting set of four nonlinear algebraic equations is given by

$$\begin{aligned}
&\tfrac{1}{2}k_{13}a_3 \sin\gamma + \tfrac{1}{2}d_{11}a_1 + \tfrac{1}{2}d_{13}a_3 \cos(\beta_3 - \beta_1) + (B/2)\sin\beta_1 = 0\\
&-\tfrac{1}{2}k_{32}a_1 \sin\gamma + \tfrac{1}{2}d_{31}a_3 + \tfrac{1}{2}d_{32}a_1 \cos(\beta_3 - \beta_1) = 0\\
&\tfrac{1}{2}k_{12}a_1 - \sigma a_1 + \tfrac{1}{2}k_{13}a_3 \cos(\beta_3 - \beta_1) + m_f(a_1/2)^m\\
&-\tfrac{1}{2}d_{13}a_3 \sin(\beta_3 - \beta_1) - (B/2)\cos\beta_1 = 0\\
&\tfrac{1}{2}k_{33}a_3 - \sigma a_3 + \tfrac{1}{2}k_{32}a_1 \cos(\beta_3 - \beta_1) + n_f(a_3/2)^n\\
&+\tfrac{1}{2}d_{32}a_1 \sin(\beta_3 - \beta_1) + \tfrac{1}{2}\lambda a_3 = 0
\end{aligned} \tag{19}$$

They are solved numerically to obtain the amplitudes and phases of the nonlinear resonances. These equations are analogous to relations (15) of the unforced, undamped case. Once the stationary values for the amplitudes and phases are computed, the steady-state responses are approximated as follows:

$$\begin{aligned}
u(t) &= a_{10}\cos[(1+\varepsilon\sigma)\alpha t + \beta_{10}] + \mathcal{O}(\varepsilon)\\
v(t) &= \mathcal{O}(\varepsilon)\\
w(t) &= a_{30}\cos[(1+\varepsilon\sigma)\alpha t + \beta_{30}] + \mathcal{O}(\varepsilon)
\end{aligned} \tag{20}$$

where subscripts 0 denote stationary values. The effectiveness of the vibration isolation is judged by the smallness of the amplitude a_{30} of the steady-state oscillation of the LSS of the system because only then is the level of transmitted vibration to the ground of Fig. 1 small.

A numerical example is performed to show the effect of nonlinear mode localization on the structure with steady-state motions near the linearized resonances. The stability of solutions is computed by finding the eigenvalues of the Jacobian matrix of the evolution equations (19). The branches of the nonlinear resonances of the system with the parameters

$$\begin{aligned}
&m = 9, \quad n = 3, \quad k = 21.0225, \quad f_1 = 1, \quad f_3 = 4\\
&m_1 = 1, \quad m_2 = 2.53554, \quad m_3 = 5.07108\\
&c_1 = 4.5, \quad c_2 = 3.5, \quad c_3 = 5.0, \quad \lambda = -8.79123\\
&\eta = 3, \quad L = -7.5, \quad B = 10, \quad \text{and} \quad \varepsilon = 0.030
\end{aligned} \tag{21}$$

are shown in Fig. 3. These curves are generated by numerically solving Eqs. (20) while varying the frequency detuning σ of the external excitation. The dotted lines represent the corresponding backbone curves[18] that depict the variation of the ratio c vs σ for the undamped, unforced case. The solid lines represent stable motions that correspond to periodic oscillations of Eqs. (1). The dashed lines represent solutions that are unstable and, thus, not physically realizable. The onset of the unstable region occurs through a saddle-node bifurcation. This system possesses a strongly localized NNM whose backbone curve originates near $\sigma = 0.84$ and a nonlocalized NNM with a backbone curve beginning near $\sigma = -2.74$.

With this example we have demonstrated that nonlinear mode localization, induced by designing a system with passive nonlinear springs, gives rise to localized steady-state motion in the frequency range close to the corresponding localized backbone curve. On this branch, the steady-state amplitude a_3 of the LSS is small, whereas the corresponding amplitude a_1 of the USS is orders of magnitude higher (magnitude of a_1 is on the same order of magnitude as would be the linear response). In the frequency range of the localized branch, the steady-state oscillations of the forced system are spatially confined mainly to the upper substructure, leading to enhanced

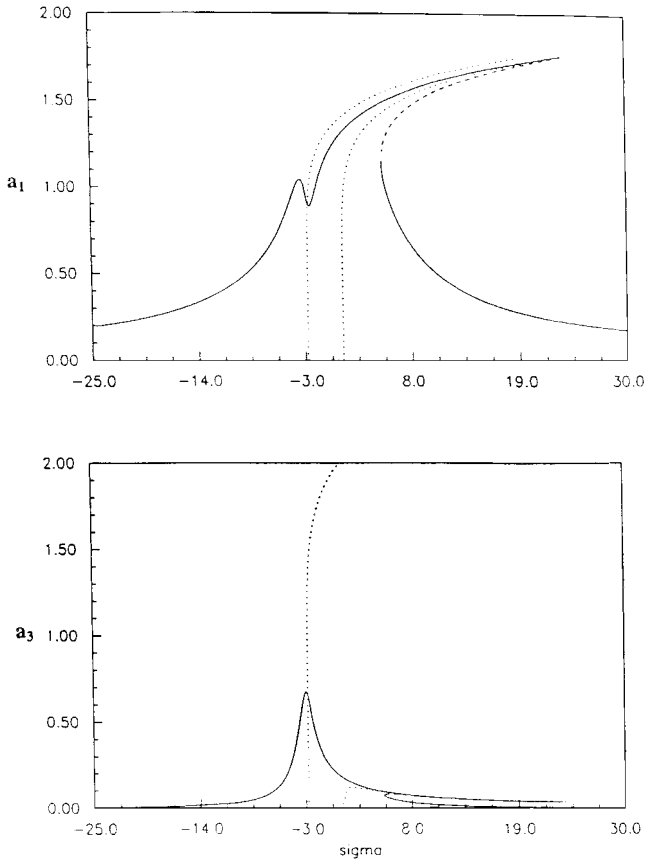

Fig. 3 Nonlinear resonances of the system with a strongly localized NNM and the parameters $m = 9$, $n = 3$, $k = 21.0225$, $f_1 = 1$, $f_3 = 4$, $m_1 = 1$, $m_2 = 2.53554$, $m_3 = 5.07108$, $c_1 = 4.5$, $c_2 = 3.5$, $c_3 = 5.0$, $\lambda = -8.79123$, $\eta = 3$, $L = -7.5$, $B = 10$, and $\varepsilon = 0.030$: solid and dashed lines denote stable and unstable quasiperiodic steady-state motions, respectively, and dotted lines indicate the backbone curves.

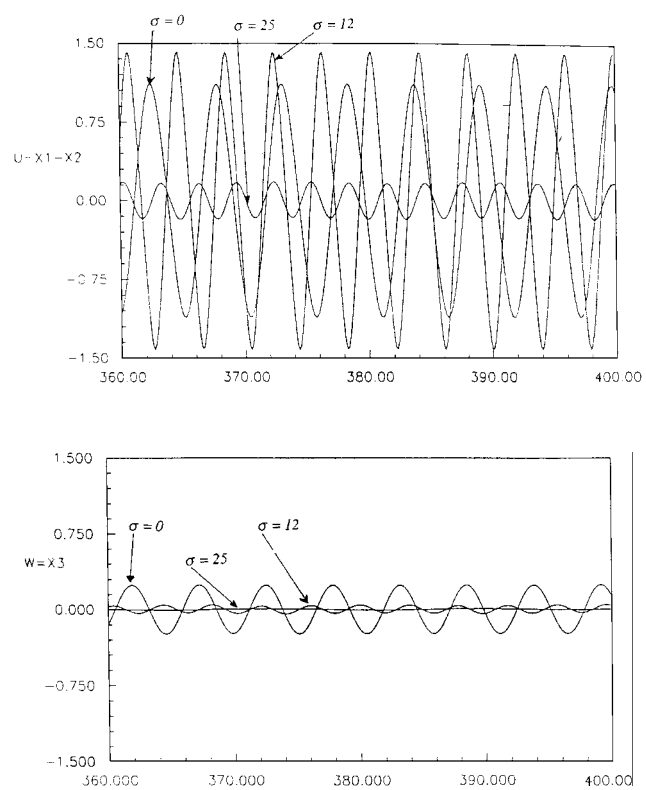

Fig. 4 Time history response for the system with the same parameters as in Fig. 3 and $\sigma = 0$, 12, and 25.

vibration isolation and therefore substantially smaller motions for the lower substructure.

To validate the perturbation analysis, the original equations of motion (1) are numerically integrated with this set of parameters and initial conditions close to the values obtained in the analysis. In Fig. 4 the time traces of displacement u and w for three different σ are shown. At $\sigma = 0$, the amplitude of a_1 begins to grow, whereas the amplitude of a_3 has begun to decay. At $\sigma = 12$, the system is at its greatest point of localization so the amplitude of a_1 is large, i.e., the USS is vibrating with the same order of magnitude as the linear system, yet the amplitude of a_3 is extremely small, as predicted by the perturbation analysis. Last, at $\sigma = 25$, a jump has already occurred, so the system has settled back to small linear motions away from resonance.

The preceding analysis proves that the system under consideration can be designed to possess localized NNMs, which, in turn, can lead to improved vibration isolation performance. In the next section we develop an optimization procedure to compute the set of system parameters, i.e., masses, dampers, and stiffnesses, that generate an optimally localized motion over a specified frequency range. The optimization analysis will be carried out using the method of harmonic balance.[19]

Optimization Analysis

To simplify the algebra involved in the analysis, we introduce a different nondimensionalization from that used earlier. Hence, considering the original Eqs. (1), we define the following nondimensional quantities:

$$\bar{x}_1 = x_1/l, \qquad \bar{x}_2 = x_2/l, \qquad \bar{x}_3 = x_3/l, \qquad \tau = \bar{\omega}t \tag{22}$$

where l is the undeformed position of mass m_3 (cf. Fig. 1) and $\bar{\omega}$ is a characteristic frequency. Substituting Eqs. (12) into Eqs. (1) and simplifying yields

$$\begin{aligned}
&\bar{x}_1'' + \frac{c_1}{m_1\bar{\omega}}(\bar{x}_1' - \bar{x}_2') + \frac{1}{lm_1\bar{\omega}^2}\hat{f}(\bar{x}_1 - \bar{x}_2) = \frac{P(\tau)}{lm_1\bar{\omega}^2}\\
&\bar{x}_2'' + \frac{c_1}{m_2\bar{\omega}}(\bar{x}_2' - \bar{x}_1') + \frac{1}{lm_1\bar{\omega}^2}\hat{f}(\bar{x}_2 - \bar{x}_1)\\
&\quad + \frac{\bar{k}}{m_2\bar{\omega}^2}(\bar{x}_2 - \bar{x}_3) + \frac{c_2}{m_2\bar{\omega}}(\bar{x}_2' - \bar{x}_3') = 0\\
&\bar{x}_3'' + \frac{c_3}{m_3\bar{\omega}}\bar{x}_3' + \frac{c_2}{m_3\bar{\omega}}(\bar{x}_3' - \bar{x}_2')\\
&\quad + \frac{1}{lm_3\bar{\omega}^2}\hat{g}(\bar{x}_3) + \frac{\bar{k}}{m_3\bar{\omega}^2}(\bar{x}_3 - \bar{x}_2) = 0
\end{aligned} \tag{23}$$

where the prime denotes the derivative with respect to the nondimensional time τ. The optimization technique is developed for the case of cubic nonlinearities, and it can be similarly extended to higher-degree nonlinearities. Thus, we assume that the nonlinear stiffnesses are given by

$$\hat{f}(y) = \bar{\alpha}_1 ly + \bar{\alpha}_3 l^3 y^3, \qquad \hat{g}(y) = \bar{\gamma}_1 ly + \bar{\gamma}_3 l^3 y^3 \tag{24}$$

Setting

$$\bar{\alpha}_1 = lm_1\bar{\omega}^2, \qquad \alpha_3 = \frac{\bar{\alpha}_3 l^2}{\bar{\alpha}_1}, \qquad \gamma_1 = \frac{m_1}{m_3}\frac{\bar{\gamma}_1}{\bar{\alpha}_1}, \qquad \gamma_3 = \frac{m_1 l^2}{m_3}\frac{\bar{\gamma}_3}{\bar{\alpha}_1} \tag{25}$$

and substituting the result into Eqs. (23), we obtain

$$\begin{aligned}
&\bar{x}_1'' + \mu_1(\bar{x}_1' - \bar{x}_2') + \bar{x}_1 - \bar{x}_2 + \alpha_3(\bar{x}_1 - \bar{x}_2)^3 = \hat{P}(\tau)\\
&\bar{x}_2'' + M_{12}\mu_1(\bar{x}_2' - \bar{x}_1') - M_{12}(\bar{x}_1 - \bar{x}_2) - M_{12}\alpha_3(\bar{x}_1 - \bar{x}_2)^3\\
&\quad + kM_{12}(\bar{x}_2 - \bar{x}_3) + \mu_2(\bar{x}_2' - \bar{x}_3') = 0\\
&\bar{x}_3'' + \mu_3\bar{x}_3' + M_{23}\mu_2(\bar{x}_3' - \bar{x}_2') + \gamma_1\bar{x}_3\\
&\quad + \gamma_3\bar{x}_3^3 + kM_{12}M_{23}(\bar{x}_3 - \bar{x}_2) = 0
\end{aligned} \tag{26}$$

where

$$M_{12} = m_1/m_2, \qquad M_{23} = m_2/m_3, \qquad k = \bar{k}/l\bar{\alpha}_4$$
$$\mu_1 = (c_1/m_1)\sqrt{m_1/\bar{\alpha}_4}, \qquad \mu_2 = (c_2/m_3)\sqrt{m_1/\bar{\alpha}_4} \tag{27}$$
$$\mu_3 = (c_3/m_3)\sqrt{m_1/\bar{\alpha}_4}$$

To further simplify the analysis, we introduce the coordinate transformations $u = \bar{x}_1 - \bar{x}_2$, $w = \bar{x}_3$, and $v = M_{12}\bar{x}_1 + \bar{x}_2$. Hence, u represents the relative motion inside the USS, v is a scaled displacement of the center of gravity of the USS, and w is the motion of the LSS. Then, the equations governing u, v, and w are given by

$$\begin{aligned}
&u'' + \left[\mu_1(1+M_{12}) + \frac{M_{12}}{1+M_{12}}\mu_2\right]u' - \frac{\mu_2}{1+M_{12}}v' + \mu_2 w' \\
&+ \left(1 + M_{12} + \frac{M_{12}^2 k}{1+M_{12}}\right)u - \frac{M_{12}k}{1+M_{12}}v + kM_{12}w \\
&+ (1+M_{12})\alpha_3 u^3 = \hat{P}(\tau) \\
&v'' - \frac{M_{12}\mu_2}{1+M_{12}}u' + \frac{\mu_2}{1+M_{12}}v' - \mu_2 w' - \frac{M_{12}^2 k}{1+M_{12}}u \\
&+ \frac{M_{12}k}{1+M_{12}}v - kM_{12}w = M_{12}\hat{P}(\tau) \\
&w'' + \frac{M_{12}M_{23}\mu_2}{1+M_{12}}u' - \frac{M_{23}\mu_2}{1+M_{12}}v' + (\mu_3 + M_{23}\mu_2)w' \\
&+ \frac{M_{23}M_{12}^2 k}{1+M_{12}}u - \frac{M_{23}M_{12}k}{1+M_{12}}v + (\gamma_1 + M_{23}M_{12}k)w + \gamma_3 w^3 = 0
\end{aligned} \tag{28}$$

Applying the method of harmonic balance,[19] we express the steady-state periodic solution of Eqs. (28) in terms of a sum of harmonics as

$$x_i = \sum_{m=1}^{N} A_{mi}\cos[m(\omega\tau + \beta_0)] \tag{29}$$

where $i = 1, 2, 3$. Substituting Eq. (29) into the equations of motion and equating the coefficients of identical harmonics to zero, we obtain a set of $m \times i$ algebraic equations governing the amplitudes A_{mi}. These equations are usually solved for ω and A_{mi} in terms of A_{11} to yield the equations that describe the steady-state response of the system.

As in the preceding section, we consider first the undamped and unforced system to determine the structure of its NNMs. Hence, we set μ_i and $\hat{P}(t) = 0$ in Eqs. (28) and consider only the first harmonic in Eq. (29) to compute a leading-order approximation to the solution. Thus, we seek a solution in the form

$$u = a_1\cos(\omega\tau) \qquad v = r_1 u \qquad w = r_2 u \tag{30}$$

We note that r_2 represents the ratio of the amplitudes of w to u, and it is the quantity that we want to minimize. The quantity r_1 represents the ratio of the amplitudes of v to u. Substituting Eqs. (30) into Eqs. (28) and equating the coefficients of $\cos(\omega\tau)$ equal to zero, we obtain the following nonlinear algebraic relations:

$$\begin{aligned}
&a_1\left[1 + M_{12} + \frac{M_{12}^2 k}{1+M_{12}} + \frac{3}{4}(1+M_{12})\alpha_3 a_1^2 \right.\\
&\left. + \frac{M_{12}k}{1+M_{12}}r_1 + M_{12}kr_2 - \omega^2\right] = 0 \\
&a_1\left[-\frac{M_{12}^2 k}{1+M_{12}} + \frac{M_{12}k}{1+M_{12}}r_1 - \omega^2 r_1 - M_{12}kr_2\right] = 0 \\
&a_1\left[\frac{M_{12}^2 M_{23}k}{1+M_{12}} - \frac{M_{12}M_{23}k}{1+M_{12}}r_1 \right.\\
&\left. + (\gamma_1 + M_{12}M_{23}k - \omega^2)r_2 + \frac{3}{4}\gamma_3 a_1^2 r_2^3\right] = 0
\end{aligned} \tag{31}$$

There are two possible solutions: $a_1 = 0$ (which is a trivial solution) and

$$r_1 = \frac{M_{12}k[M_{12} + (1+M_{12})r_2]}{M_{12}k - (1+M_{12})\omega^2} \tag{32a}$$

$$a_1^2 = \frac{4}{3}\frac{M_{12}k - [1 + M_{12}(1+k) - \omega^2 + M_{12}kr_2]\omega^2}{\alpha_3[(1+M_{12})\omega^2 - M_{12}k]} \tag{32b}$$

where r_2 is governed by

$$\begin{aligned}
&\{\gamma_1\omega^2 - \omega^4(1+M_{12}) + [M_{12}(\omega^2 - \gamma_1) + M_{23}(1+M_{12})]k\}r_2 \\
&+ (\gamma_3/\alpha_3)\{M_{12}k - [1 + M_{12}(1+k)]\omega^2\}r_2^3 \\
&- (\gamma_3/\alpha_3)M_{12}k\omega^2 r_2^4 + M_{12}^2 M_{23}k\omega^2 = 0
\end{aligned} \tag{32c}$$

Equations (32a) and (32b) can be used to compute the ratio r_1 and the amplitude a_1 as functions of the frequency ω. Equation (32c) governs the dependence of the ratio r_2 on the frequency and the system parameters. The design objective is to minimize the transfer of energy from the USS to the LSS of the system or, equivalently, to minimize the ratio r_2. Hence, to induce the optimal localization properties into the system, one needs to minimize the number and magnitudes of the real roots of Eq. (32c) over a specified frequency range. Minimizing the number of real roots minimizes the number of NNMs and, thus, the number of nonlinear resonance branches.

In what follows, we apply the method of constrained variation[20] to minimize the quantity

$$f = \sum_{i=1}^{N}[r_{2i}(\omega_i)]^2 \tag{33}$$

where the r_{2i} are solutions of Eq. (32c) at the discrete frequencies ω_i where the optimization is performed. The parameters k, α_3, M_{ij}, and γ_i in Eq. (32c) are considered as the design variables whose values are computed by the optimization routine, whereas the variable ω represents the frequency at which the optimization is performed. The optimization is performed using the IMSL routine DNCONF[21] that employs the successive quadratic programming method developed by Schittkowski.[22] The constraint equation (32c) is nonlinear and results in a plethora of locally minimal optimized solutions. These local minima depend on the initial guesses and may not reflect the best global optimization possible. Hence, to increase the probability of finding a true optimized result, random sets of initial guesses are generated and used to start the optimization routine. In Table 1, the results of three such optimization runs are summarized. Cases 1 and 2 represent fairly good optimization results, and case 3 represents a poor result.

Although a formal sensitivity analysis is not performed, the authors note that the small optimized value of kM_{12} is consistent with previous works on linear and nonlinear localization where it was found that a prerequisite for localization in a system composed of substructures is weak coupling stiffness. The NNMs of the unforced and undamped system of case 2 are depicted in Fig. 5 as functions of the frequency. For $\omega < 1.0788$, Eqs. (35) possess only the trivial solution. At $\omega = 1.0788$, a bifurcation occurs and the two NNMs depicted in Fig. 5 develop. Similar curves were generated for cases 1 and 3, but in the interest of space are omitted. The differences in magnitude of the NNMs for cases 1–3 are the same as those predicted by the value of f in the optimization.

Table 1 Optimization results with f minimized at four discrete frequencies; ω_i = 1.00, 1.1, 1.2, 1.5

Parameter	Lower bound	Upper bound	Results Case 1	Case 2	Case 3
kM_{12}	0.00001	10.0	0.0001430	0.0001	1.31722
M_{12}	0.1	3.0	0.12001	0.16389	0.1000
M_{23}	0.1	100.0	28.3284	18.1690	0.1000
γ_1	0.1	100.0	187.6287	95.2359	172.6641
γ_3/α_3	−60.0	60.0	−35.6760	6.51466	4.23117
f			0.2248	0.2942	0.3975
			$\times 10^{-10}$	$\times 10^{-12}$	$\times 10^{-4}$

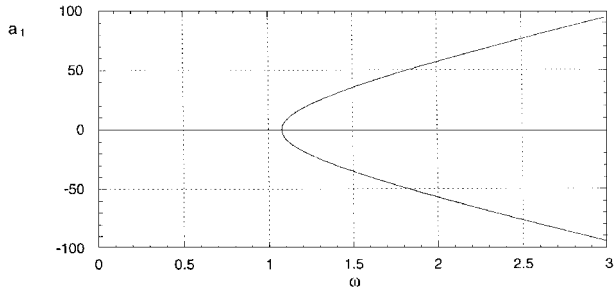

a) Amplitude of a_1

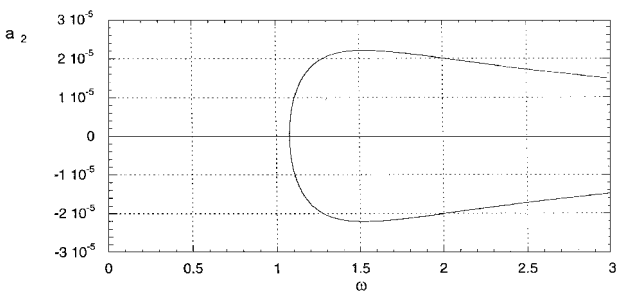

b) Amplitude of a_2

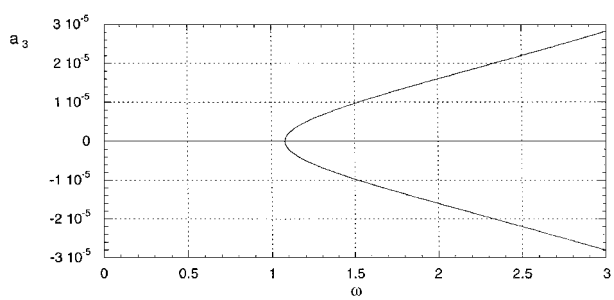

c) Amplitude of a_3

Fig. 5 Backbone curves of the unforced and undamped system of case 2.

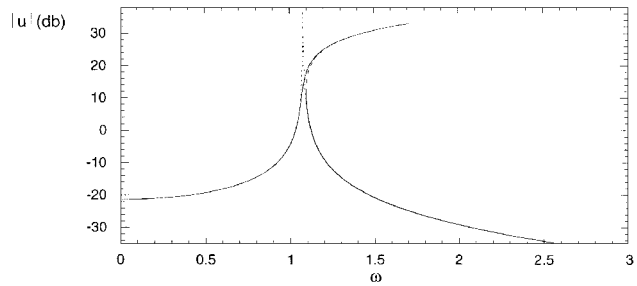

a) Magnitude of u in dB

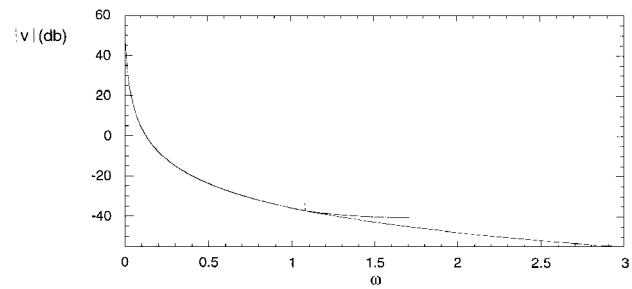

b) Magnitude of v in dB

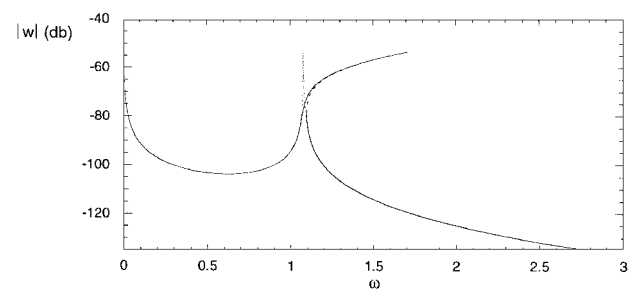

c) Magnitude of w in dB

Fig. 6 Resonance curves of the forced and damped system with parameters of case 2 and $F = 0.1$, $\mu_1 = 0.001$, $\mu_2 = 0.001$, and $\mu_3 = 0.001$; solid and dashed lines denote stable and unstable steady-state motions, respectively, and dotted lines represent the corresponding linear response.

After optimizing the NNMs and inducing optimal localization properties, we compute the steady-state responses of the optimized system by considering Eqs. (28) with $\mu_i \neq 0$ and $\hat{P}(\tau) = F\cos(\omega\tau)$. Assuming a solution of the form

$$\begin{aligned} u &= a_1\cos(\omega\tau) + b_1\sin(\omega\tau) \\ v &= a_2\cos(\omega\tau) + b_2\sin(\omega\tau) \\ w &= a_3\cos(\omega\tau) + b_3\sin(\omega\tau) \end{aligned} \tag{34}$$

(where the sine and cosine terms are used due to the presence of damping), substituting into Eqs. (28), and equating the coefficients of $\cos(\omega\tau)$ and $\sin(\omega\tau)$ to zero, we obtain the following algebraic equations, which are analogous to the unforced, undamped relations (31):

$$\begin{aligned}
&a_1\left(1 + M_{12} + \frac{kM_{12}^2}{1+M_{12}} - \omega^2\right) - a_2\frac{kM_{12}}{1+M_{12}} \\
&\quad + b_1\left[\mu_1(1+M_{12}) + \frac{\mu_2 M_{12}}{1+M_{12}}\right]\omega + a_3 kM_{12} + b_2\frac{\mu_2\omega}{1+M_{12}} \\
&\quad + b_3\mu_2\omega + \frac{3}{4}\alpha_3(1+M_{12})(a_1^3 + a_1 b_1^2) - F = 0 \\
&-a_1\left[\mu_1(1+M_{12}) + \frac{\mu_2 M_{12}}{1+M_{12}}\right]\omega + a_2\frac{\mu_2\omega}{1+M_{12}} \\
&\quad + b_1\left(1 + M_{12} + \frac{kM_{12}^2}{1+M_{12}} - \omega^2\right) - a_3\mu_2\omega + b_2\frac{kM_{12}}{1+M_{12}} \\
&\quad + b_3 kM_{12} + \frac{3}{4}\alpha_3(1+M_{12})(b_1^3 + a_1^2 b_1) = 0 \\
&-a_1\frac{kM_{12}^2}{1+M_{12}} + a_2\frac{kM_{12}}{1+M_{12}} - a_3 kM_{12} - b_1\frac{\mu_2 M_{12}}{1+M_{12}}\omega \\
&\quad + b_2\frac{\mu_2}{1+M_{12}}\omega - b_3\mu_3\omega - M_{12}F = 0 \\
&a_1\frac{\mu_2 M_{12}}{1+M_{12}}\omega - a_2\frac{\mu_2}{1+M_{12}}\omega + a_3\mu_3\omega - b_1\frac{kM_{12}^2}{1+M_{12}} \\
&\quad + b_2\frac{kM_{12}}{1+M_{12}} - b_3 kM_{12} = 0 \\
&a_1\frac{kM_{12}^2 M_{23}}{1+M_{12}} - a_2\frac{kM_{12}M_{23}}{1+M_{12}} + a_3(\gamma_1 + kM_{12}M_{23} - \omega^2) \\
&\quad + b_1\frac{\mu_2 M_{12}M_{23}}{1+M_{12}}\omega - b_2\frac{\mu_2 M_{23}}{1+M_{12}}\omega + b_3(\mu_3 + \mu_2 M_{23})\omega \\
&\quad + \frac{3}{4}\gamma_3(a_3^3 + a_3 b_3^2) = 0 \\
&-a_1\frac{\mu_2 M_{12}M_{23}}{1+M_{12}}\omega + a_2\frac{\mu_2 M_{23}}{1+M_{12}}\omega - a_3(\mu_3 + \mu_2 M_{23})\omega \\
&\quad + b_1\frac{kM_{12}^2 M_{23}}{1+M_{12}} - b_2\frac{kM_{12}M_{23}}{1+M_{12}} + b_3(\gamma_1 + kM_{12}M_{23} - \omega^2) \\
&\quad + \frac{3}{4}\gamma_3(b_3^3 + a_3^2 b_3) = 0
\end{aligned} \tag{35}$$

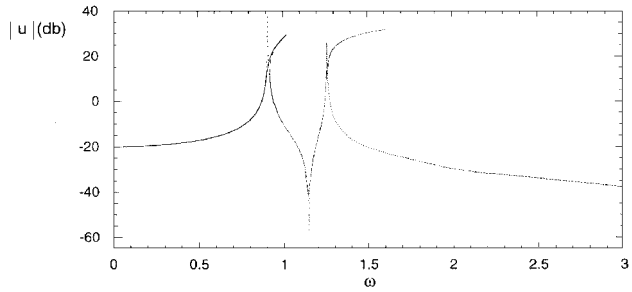

a) Magnitude of u in dB

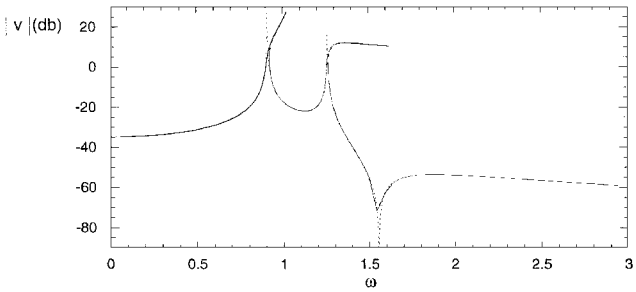

b) Magnitude of v in dB

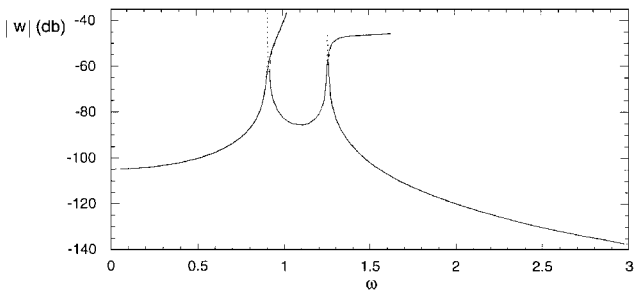

c) Magnitude of w in dB

Fig. 7 Resonance curves of the forced and damped system with parameters of case 3 and $F = 0.1$, $\mu_1 = 0.001$, $\mu_2 = 0.001$, and $\mu_3 = 0.001$; solid and dashed lines denote stable and unstable steady-state motions, respectively, and dotted lines represent the corresponding linear response.

These equations were solved numerically with the parameters listed in Table 1 and $\alpha_3 = 0.001$, $F = 0.1$, $\mu_1 = 0.001$, $\mu_2 = 0.001$, and $\mu_3 = 0.001$. The stability of the solutions was obtained using Hill's infinite determinant.[19] The forced response of the system for case 2 is shown in Fig. 6, where the solid-dashed line represents the nonlinear response, and the dashed line represents the linear response. Similarly, the forced response of case 3 is shown in Fig. 7. For all cases, the amplitude of w is orders of magnitude smaller than that of u or v (notice that the vertical scale in the plots is in decibels). In addition, the effect of the nonlinearity is to attenuate the maximum amplitudes of the linear resonances.

Finally, to verify that the use of a single harmonic expansion is sufficient for capturing the dynamics of the system, we numerically integrated Eqs. (28) with initial conditions identical to the theoretical predictions for steady-state motions corresponding to case 2. The integration was performed using a fifth-order Runge–Kutta[23] with error tolerance set to 1×10^{-12} and an adaptive time step. The amplitudes of the responses in each case are nearly those predicted by the single-harmonic expansion, and in addition, the frequency content of the numerical time responses appear to contain only one harmonic. These results indicate that the use of a single harmonic in the theoretical analysis is justified. The results of one of the numerical integrations is presented in Fig. 8. The initial conditions used correspond to $\omega = 1.5002$ with initial conditions on the unstable branch. We expect the solution shown to be unstable, and the simulation agrees with our theoretical prediction. In fact, had we allowed the integration to proceed for a longer time, the response would have settled to that of the lower stable branch.

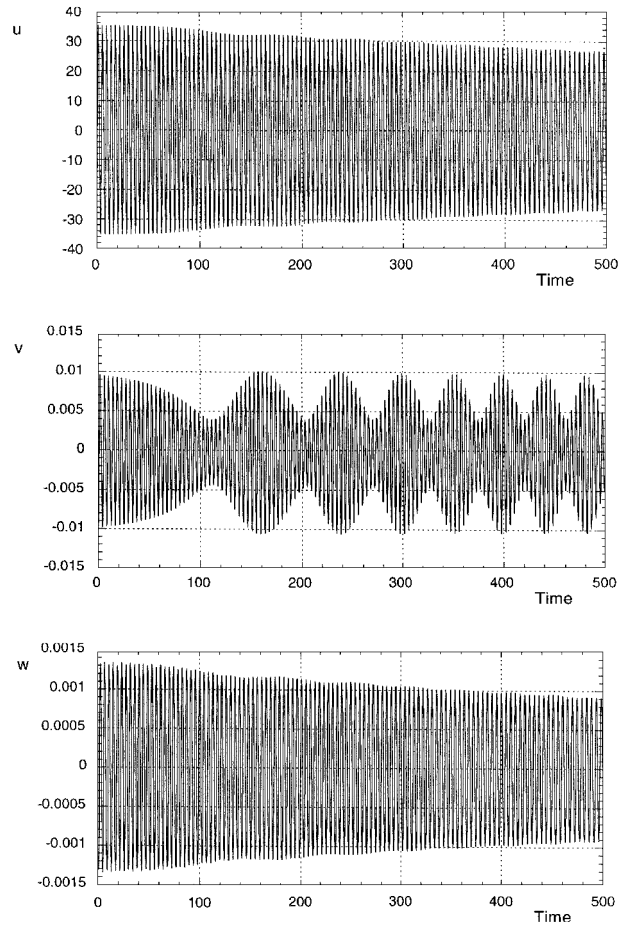

Fig. 8 Unstable steady-state response of the system with parameters of case 2, $\omega = 1.5002$, and initial conditions on the unstable branch (cf. Fig. 8).

Conclusions

In this study, we have shown that the use of nonlinear stiffnesses can greatly enhance the vibration isolation properties of a passive mechanical isolator. Indeed, such a system can be designed to possess stable localized NNMs with most of their energy confined to a predetermined subsystem, away from the main body that needs to be isolated. When isolators with localized NNMs are subjected to harmonic excitations, in certain frequency ranges, the resulting resonances become similarly localized, and the level of transmitted undesirable vibrations is greatly reduced. Hence, nonlinear localization can provide a valuable tool for developing improved vibration and shock isolation designs, otherwise unattainable using linear stiffness elements. In addition, we have developed a new design technique to optimize systematically the localized NNMs of the isolator. This is performed by localizing the vibrational energy of the isolator in a way that is compatible and beneficial to the vibration isolation objectives. Following the outlined optimization procedure, we alter the solution space describing the dynamics and ensure minimal transfer of unwanted disturbances.

Acknowledgments

Support for this work was provided in part by a National Science Foundation (NSF) Young Investigator Award (A. F. Vakakis) and by Hughes Aircraft Company, El Segundo, California. Devendra Garg is the NSF Grant Monitor. The authors would like to thank David Augenstein and John Kelly of Hughes Aircraft Company for their help with the formulation of the problem and for valuable discussions on various aspects of this work. In addition, the authors would like to thank Mohammed Fakir Abdul-Azeez of the University of Illinois at Urbana–Champaign for his valuable help in the optimization computations.

References

[1]Harris, J. A., "Design Principles for Vibration Isolation and Damping with Elastomers Including Nonlinearity," *Rubber Chemistry and Technology*, Vol. 62, 1989, pp. 515–528.

[2]Nashif, A. D., Jones, D. I. G., and Henderson, J. P., *Vibration Damping*, Wiley, New York, 1985.

[3]White, R. G., and Walker, J. G. (eds.), *Noise and Vibration*, Ellis Horwood, Chichester, England, UK, 1982.

[4]Harris, C. M. (ed.), *Shock and Vibration Handbook*, McGraw–Hill, New York, 1988.

[5]Herzog, R., "Active Versus Passive Vibration Absorbers," *Journal of Dynamic Systems, Measurement and Control*, Vol. 116, 1995, pp. 367–371.

[6]Soom, A., and Lee, M.-S., "Optimal Design of Linear and Nonlinear Vibration Absorbers for Damped Systems," *Journal of Vibration, Acoustics, Strees, and Reliability in Design*, Vol. 105, 1983, pp. 112–119.

[7]Olgac, N., and Holm-Hansen, B., "Tunable Active Vibration Absorber: The Delayed Resonator," *Journal of Dynamic Systems, Measurement and Control*, Vol. 117, 1995, pp. 513–519.

[8]Kanestrom, R. K., and Egeland, O., "Maximum Power Absorption with Active Struts," *Journal of Guidance, Control, and Dynamics*, Vol. 18, No. 4, 1995, pp. 907, 908.

[9]Inaudi, J. A., and Kelly, J. M., "Optimum Damping in Linear Isolation Systems," *Earthquake Engineering and Structural Dynamics*, Vol. 22, 1993, pp. 583–598.

[10]Vakakis, A. F., "Nonsimilar Normal Oscillations in a Strongly Nonlinear Discrete System," *Journal of Sound and Vibration*, Vol. 158, 1992, pp. 341–361.

[11]Vakakis, A. F., Manevitch, L. I., Mikhlin, Y. V., Pilipchuck, V. N., and Zevin, A. A., *Normal Modes and Localization in Nonlinear Systems*, Wiley Interscience, New York, 1996.

[12]King, M. E., and Vakakis, A. F., "An Energy-Based Approach for Computing Resonant Nonlinear Normal Modes," *Journal of Applied Mechanics*, Vol. 63, No. 3, 1996, pp. 810–819.

[13]Vakakis, A. F., and Cetinkaya, C., "Mode Localization in a Class of Multi-Degree-of-Freedom Nonlinear Systems with Cyclic Symmetry," *Journal of Applied Mathematics*, Vol. 53, 1993, pp. 265–282.

[14]Vakakis, A. F., Nayfeh, T., and King, M. E., "A Multiple-Scales Analysis of Nonlinear Localized Modes in a Cyclic Periodic System," *Journal of Applied Mechanics*, Vol. 60, No. 2, 1993, pp. 388–397.

[15]Vakakis, A. F., "Passive Spatial Confinement of Impulsive Excitations in Coupled Nonlinear Beams," *AIAA Journal*, Vol. 32, No. 9, 1994, pp. 1902–1910.

[16]Shaw, S. W., and Sharif-Bakhtiar, M., "Effects of Nonlinearities and Damping on the Dynamic Response of a Centifugal Pendulum Vibration Absorber," *Journal of Vibration and Acoustics*, Vol. 114, 1992, pp. 305–311.

[17]Shaw, S. W., Shaw, J., and Haddow, A., "On the Dynamic Response of the Nonlinear Vibration Absorber," *International Journal of Nonlinear Mechanics*, Vol. 24, 1989, pp. 281–293.

[18]Nayfeh, A. H., *Introduction to Perturbation Methods*, Wiley, New York, 1982.

[19]Nayfeh, A. H., and Mook, D. T., *Nonlinear Oscillations*, Wiley, New York, 1979.

[20]Rao, S. S., *Optimization: Theory and Applications*, 2nd ed., Wiley, New York, 1984.

[21]IMSL, *Math Library: Fortran Subroutines for Mathematical Applications*, International Mathematical and Statistical Libraries, 1989.

[22]Schittkowski, K., "NLPQL: A Fortran Subroutine Solving Constrained Nonlinear Programming Problems," *Annals of Operations Research*, Vol. 5, 1986, pp. 485–500.

[23]Press, W. H., Teukolsky, S. A., Vellerling, W. T., and Flannery, B. P., *Numerical Recipes in Fortran: The Art of Scientific Computing*, 2nd ed., Cambridge Univ. Press, New York, 1992.

A. D. Belegundu
Associate Editor